NPN Regularization For Imaging Inverse Problems

Learning null-space components for regularizing inverse problems in imaging

Jacome*, Gualdrón-Hurtado*, Suarez, Arguello. (2025). NPN: Non-Linear Projections of the Null-Space for Imaging Inverse Problems. *Advances in Neural Information Processing Systems*.
* Equal contribution.

Inverse Problems and Null-Space

$\mathbf{y}$

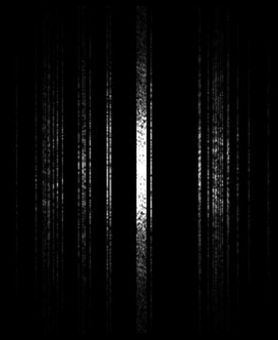

$=$

$\mathbf{H}$

$\mathbf{x}^*$

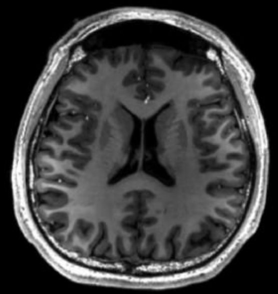

Consider:

$\mathbf{S}$

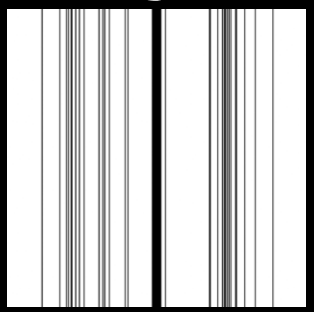

$\perp$

$\mathbf{H}$

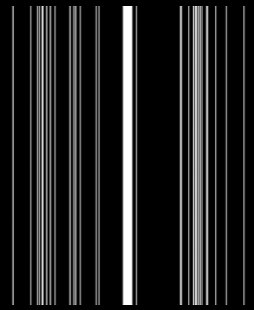

Can we recover $\mathbf{Sx}^*$ (*blind signal components to* $\mathbf{H}$) only from $\mathbf{y}$?

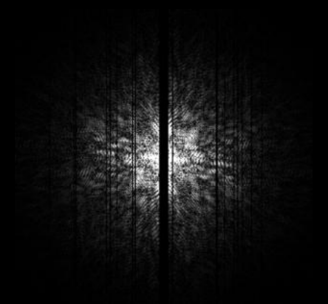

Subset of Null-space

Estimating directly the image (Traditional approaches)

Estimating directly null-space components

$\mathbf{S}\mathbb{E}[\mathbf{x}|\mathbf{y}]$ | $||\mathbf{S}\mathbb{E}[\mathbf{x}|\mathbf{y}] - \mathbf{Sx}^*||$ | $\mathbb{E}[\mathbf{Sx}|\mathbf{y}]$ | $||\mathbb{E}[\mathbf{Sx}|\mathbf{y}] - \mathbf{Sx}^*||$

Unlimited #Training samples

Limited #Training samples (Practical applications)

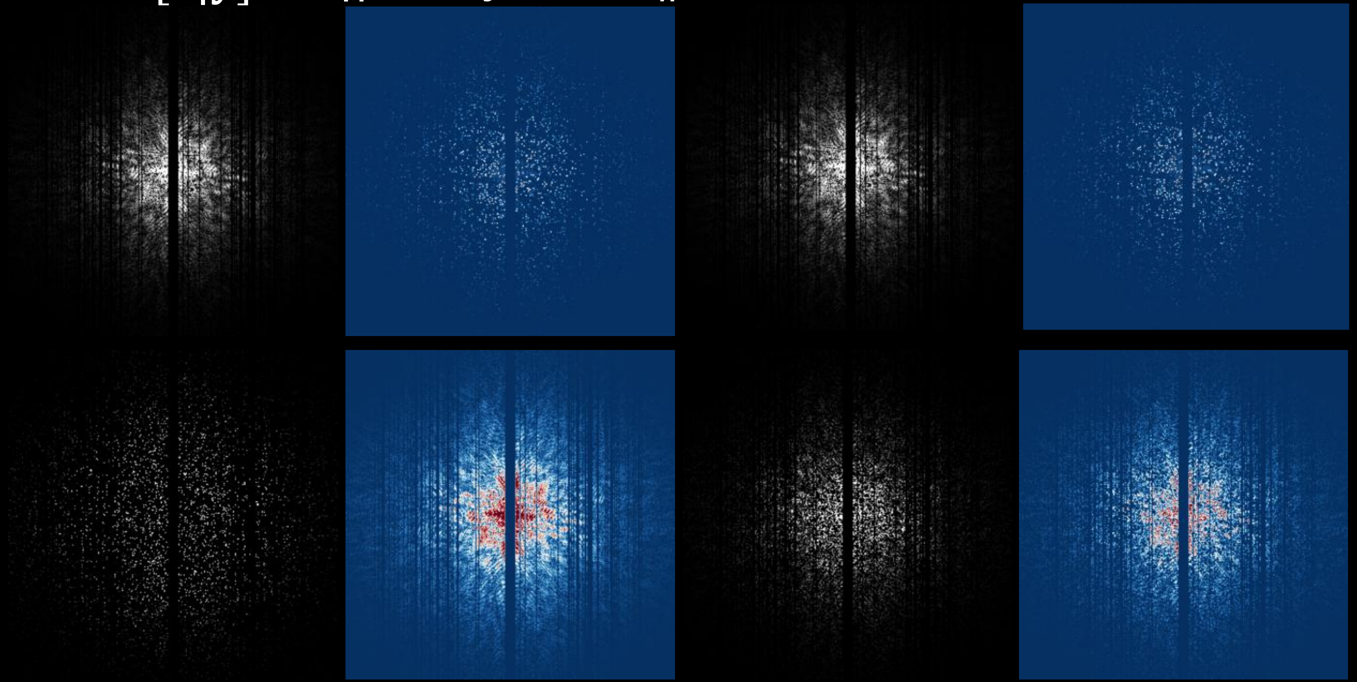

Conclusion

When the #Training samples is **limited**

Accurate estimation with $\mathbb{E}[\mathbf{x}|\mathbf{y}]$ or $\mathbb{E}[\mathbf{Sx}|\mathbf{y}]$

It is better to estimate $\mathbb{E}[\mathbf{Sx}|\mathbf{y}]$.

We propose to estimate $\mathrm{G}^*(\mathbf{y}) \approx \mathbf{Sx}^*$

Learned Null-Space Regularizer

$$\phi(\mathbf{x}) = ||\mathrm{G}^*(\mathbf{y}) - \mathbf{Sx}||$$

Accurate estimation **only** with $\mathbb{E}[\mathbf{Sx}|\mathbf{y}]$

Main issue: High dimensionality of $\mathbf{x}$

It can be used in any solver: PnP, DM, DIP...

Inverse Problems and Null-Space

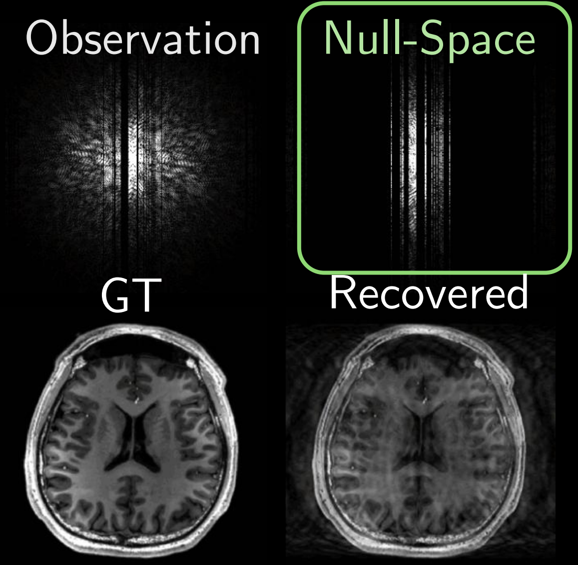

Solution on image prior

$$\hat{\mathbf{x}} = \underset{\tilde{\mathbf{x}}}{\operatorname{argmin}} \frac{1}{2}||\mathbf{y} - \mathbf{H}\tilde{\mathbf{x}}||_{\mathbf{2}}^{\mathbf{2}} + \lambda h(\tilde{\mathbf{x}}) + \gamma \frac{1}{2}||\mathrm{G}^{*}(\mathbf{y}) - \mathbf{S}\tilde{\mathbf{x}}||_{2}^{2}$$

Solution in range-space

Solution in **selected null-space**

$\mathbf{Sx}$ → Null-Space components $\mathrm{span}(\mathbf{S}^{\boldsymbol{T}}) \subset \mathrm{Null}(\mathbf{H})$

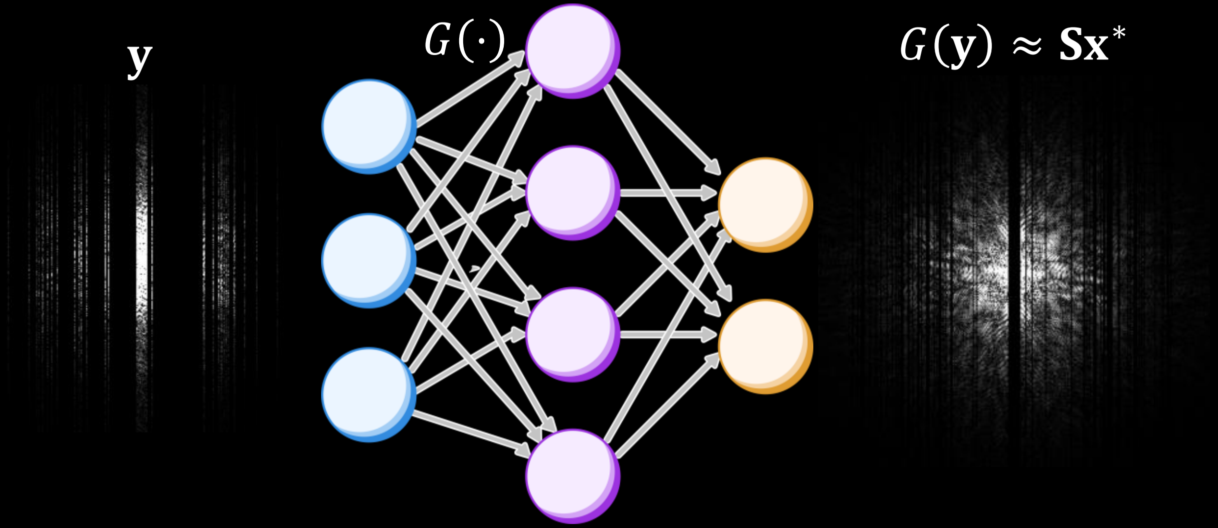

We propose to learn a regularization over blind image components to the sensing matrix

Null-Space Regularization

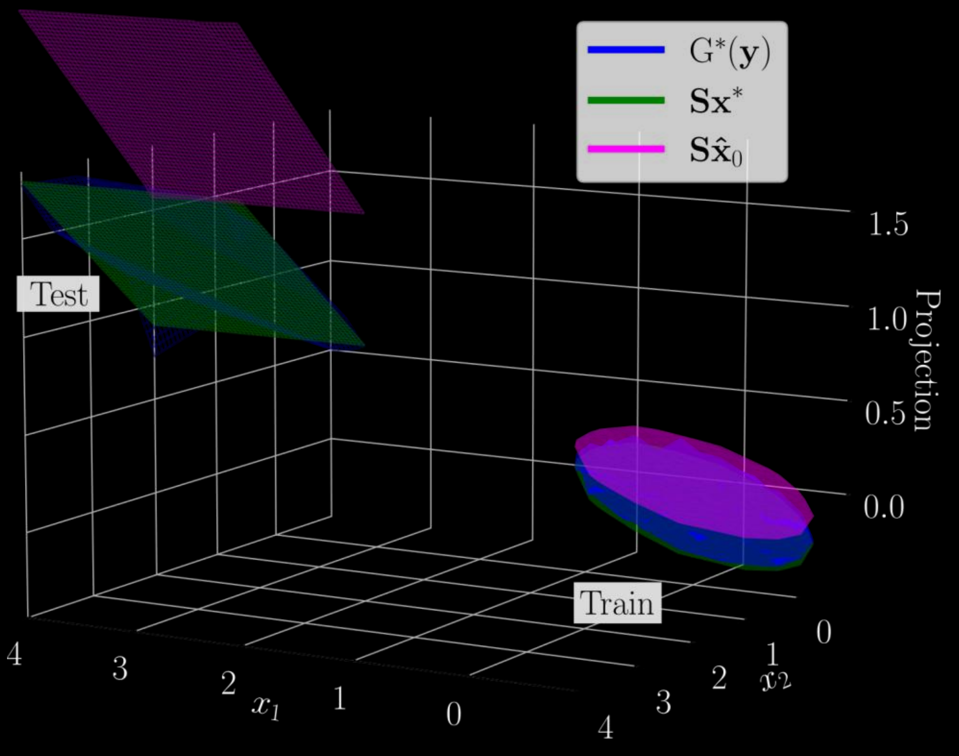

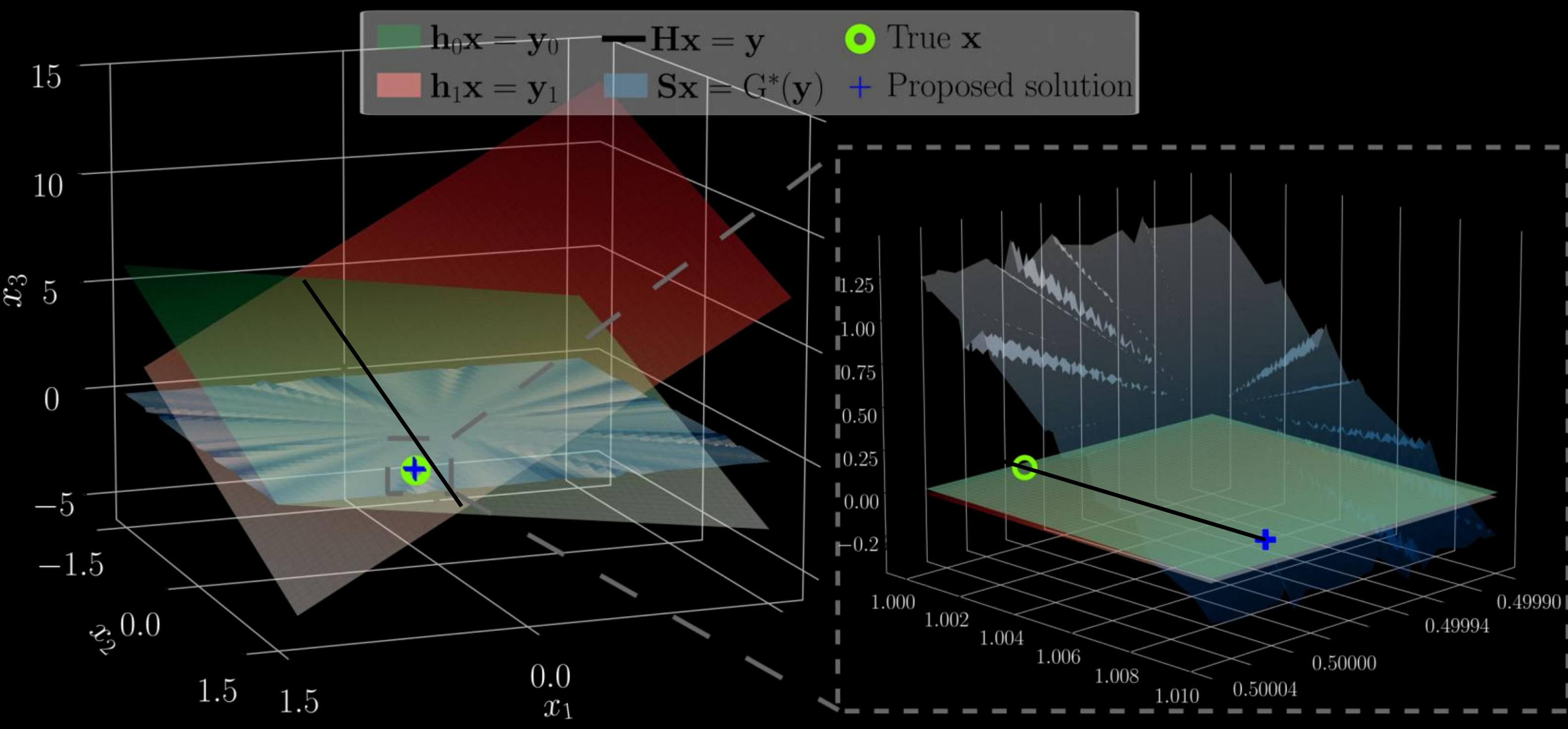

Low-dimensional learning provides better generalization

The regularization acts in a orthogonal direction to the data-fidelity

Learning Null-Space Component

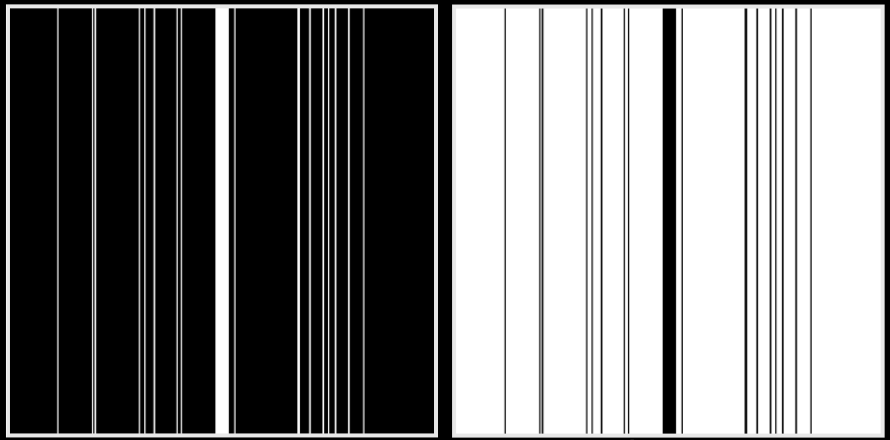

MRI Sampling Mask

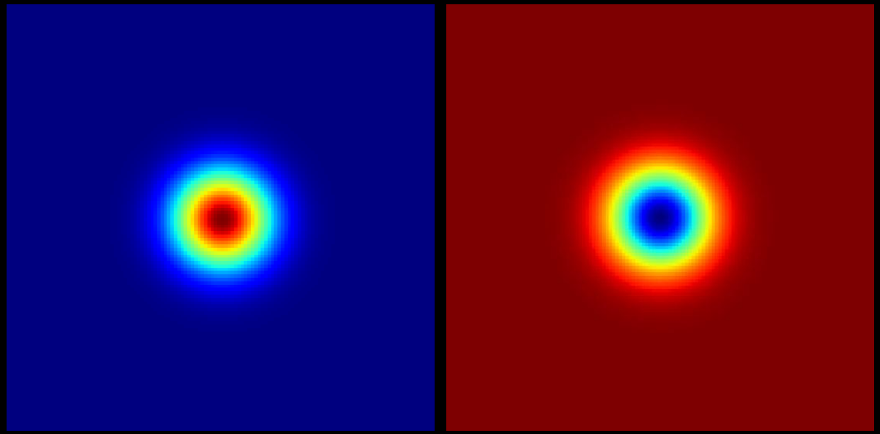

Blur Transfer Function

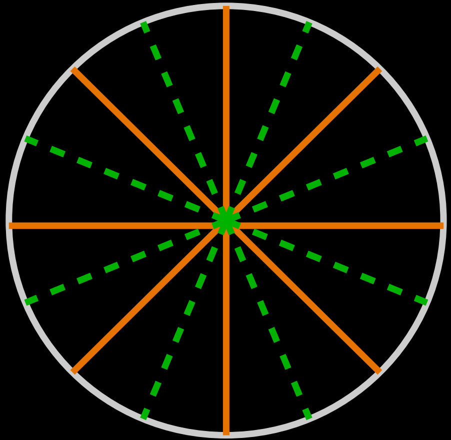

CT Acquisition Angles

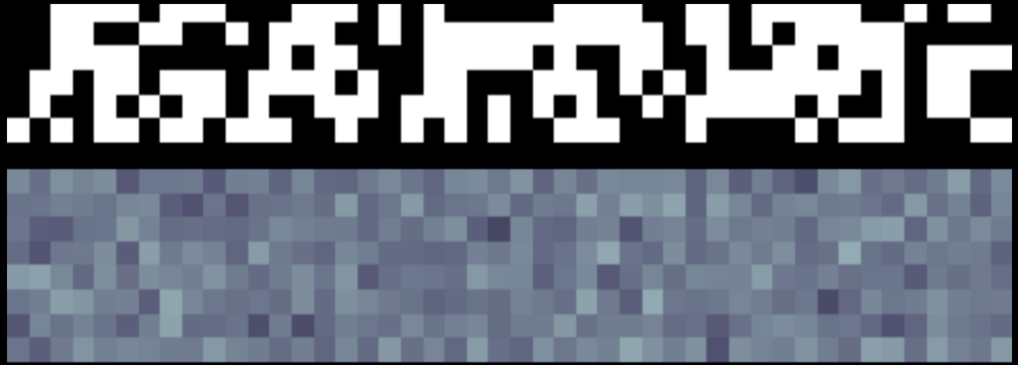

Bernoulli CS matrices

<u>Joint learning of **S** and G</u>

$$G^*, S = \underset{G,\tilde{\mathbf{S}}}{\arg\min}\, \mathbb{E}_x \left|\left|G(\mathbf{y}) - \tilde{\mathbf{S}}\mathbf{x}\right|\right| + \lambda_1 \left|\left|\mathbf{I} - \mathbf{A}^{\mathbf{T}}\mathbf{A}\right|\right| + \lambda_1 \left|\left|\mathbf{x} - \mathbf{A}^{\mathbf{T}}\mathbf{A}\mathbf{x}\right|\right|$$

Fitting Null-Space component

Ensuring orthogonality between **H** and **S**

Ensuring invertibility in the dataset subspace

$$\mathbf{A} = \begin{bmatrix} \mathbf{H} \\ \tilde{\mathbf{S}} \end{bmatrix}$$

Theoretical Advantages (PnP)

FISTA-PnP

$$\hat{\mathbf{x}} = \arg\min_{\tilde{\mathbf{x}}} ||\mathbf{y}-\mathbf{H}\tilde{\mathbf{x}}||_2^2 + \lambda h(\tilde{\mathbf{x}}) + \gamma||\mathrm{G}^*(\mathbf{y}) - \mathbf{S}\tilde{\mathbf{x}}||_2^2 \to \mathrm{x}^{\ell+1} = \mathcal{D}\left(\mathbf{x}^\ell - \alpha\left(\mathbf{H}^\mathbf{T}(\mathbf{H}\mathbf{x}^\ell - \mathbf{y}) + \gamma\mathbf{S}^\mathbf{T}\left(\mathbf{S}\mathbf{x}^\ell - \mathrm{G}^*(\mathbf{y})\right)\right)\right)$$

Convergence improvement zone

Iterations in which the null-space predictor outperforms projecting the iterate reconstruction in the null-space

$$\mathcal{L} = \left\{\ell : ||\mathrm{G}^*(\mathbf{y}) - \mathbf{S}\mathbf{x}^*|| < \left|\left|\mathbf{S}\mathbf{x}^\ell - \mathbf{S}\mathbf{x}^*\right|\right|\right\}$$

Th. 1: PnP-NPN Convergence: For $\ell \in \mathcal{L}$, the residual $||\mathbf{x}^{\ell+1} - \mathbf{x}^*||$ decay linearly with rate

Small as $\mathbf{H} \perp \mathbf{S}$

$$\rho \triangleq (1+\delta)\left(\left\|I - \alpha\left(\mathbf{H}^T\mathbf{H} + \mathbf{S}^T\mathbf{S}\right)\right\| + \left(1 + \Delta_M^S\right)\|\mathbf{S}\|\right)$$

Upper bound of G^* estimation error

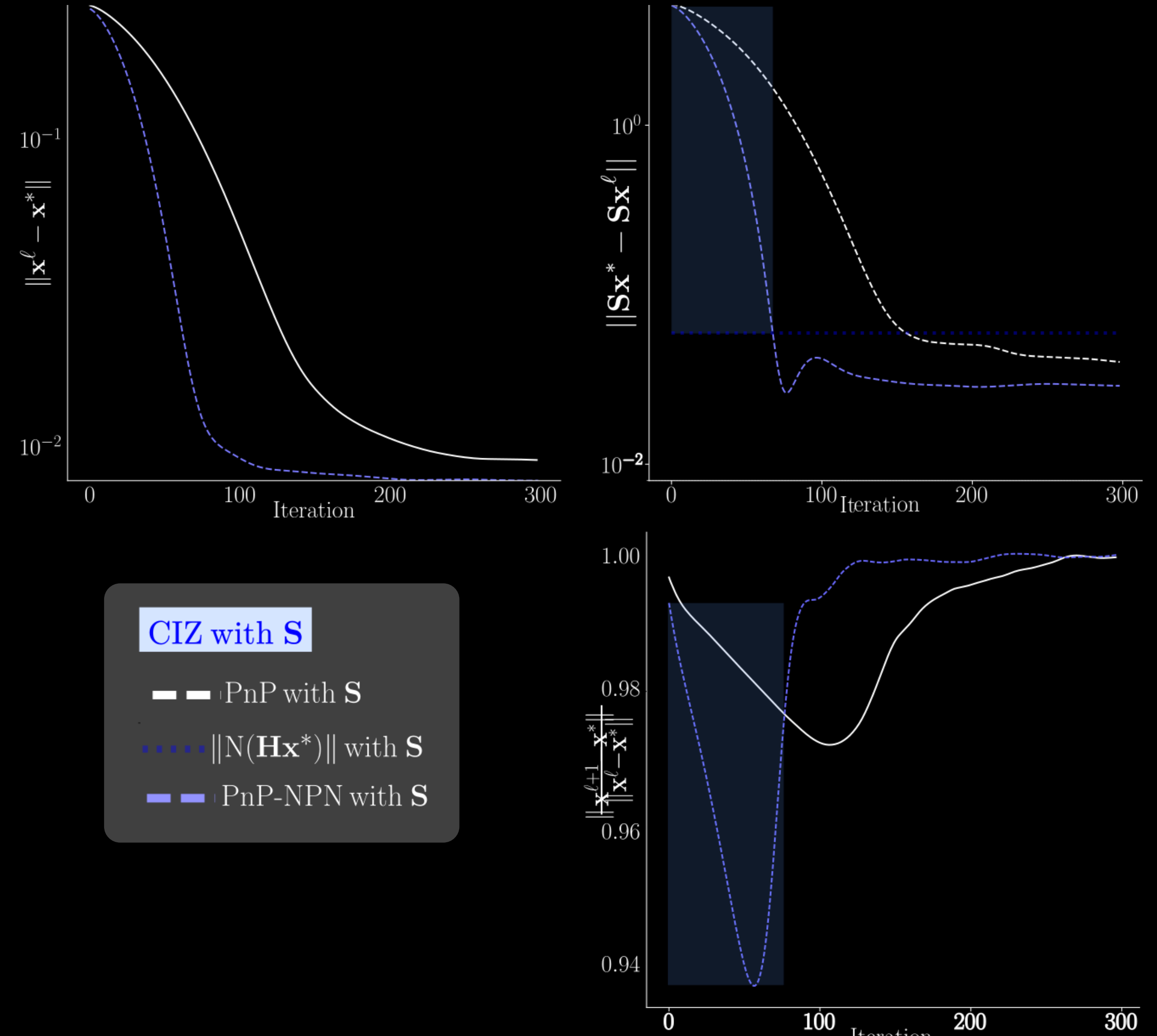

Results

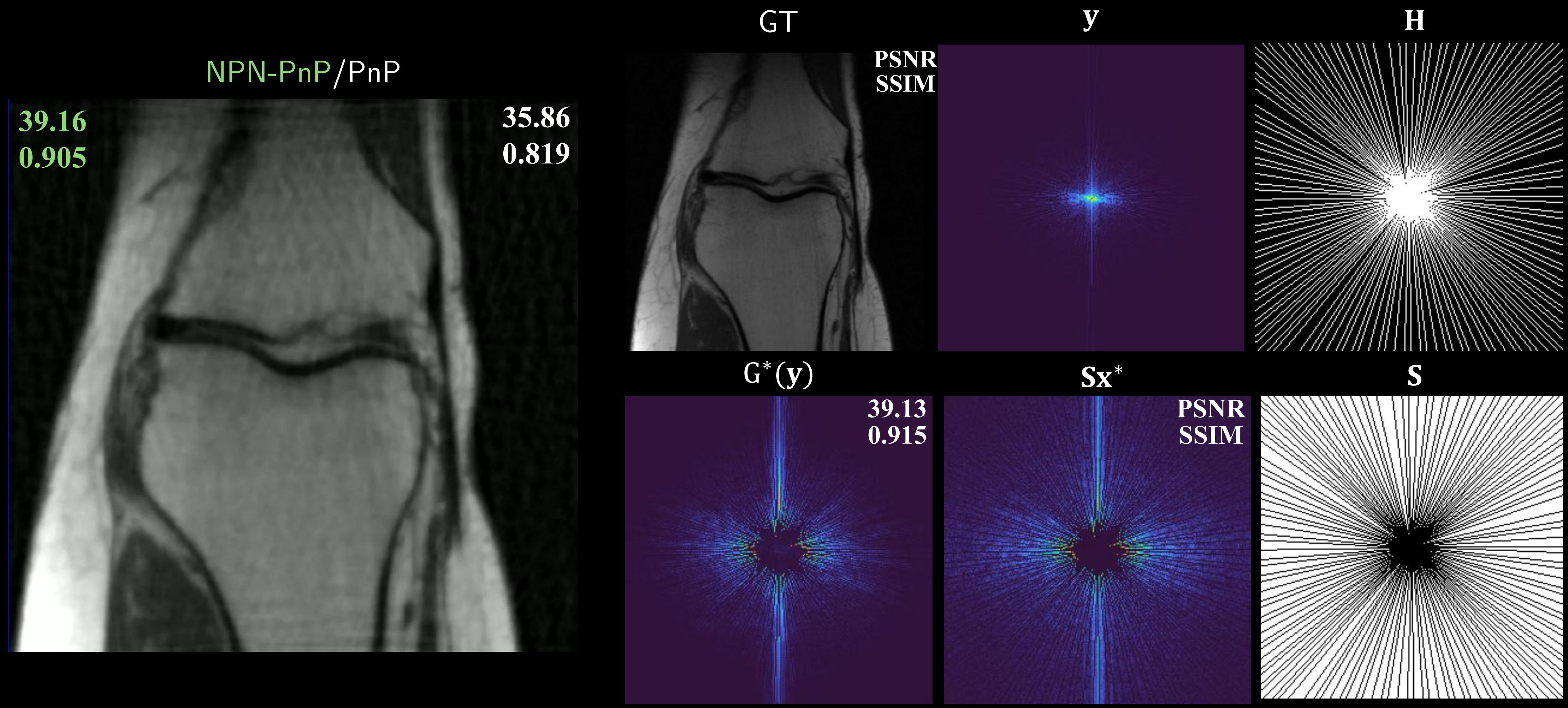

NPN-PnP/PnP
39.16
0.905
35.86
0.819
GT
PSNR
SSIM
y
H
G*(y)
39.13
0.915
Sx*
PSNR
SSIM
S

Results

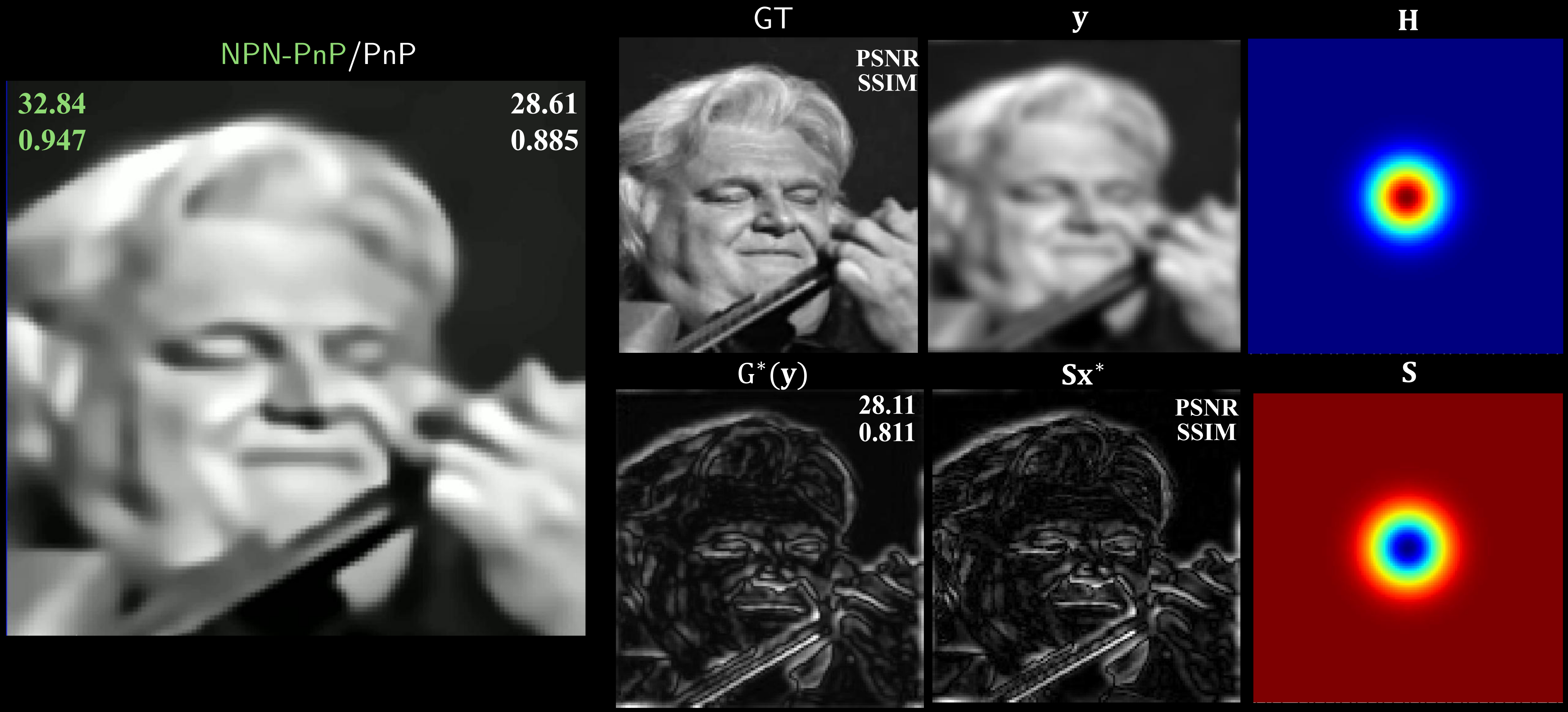
NPN-PnP/PnP
32.84
0.947
28.61
0.885
GT
PSNR
SSIM
y
H
G*(y)
28.11
0.811
Sx*
PSNR
SSIM
S

Results

Unrolling Models

Method	p/n	CIFAR-10		STL10	
		PnP	Unrolling	PnP	Unrolling
Baseline	0.0	20.04	24.32	20.09	18.35
NPN	0.1	21.12	28.53	19.91	19.64
	0.3	21.07	28.75	**21.14**	20.23
	0.5	20.78	27.64	20.77	18.76
	0.7	20.09	26.73	20.31	18.45
	0.9	20.41	**29.90**	21.02	19.48

Improvements of up to 4 dB in Unrolling Models and generalization to data distributions shift at test-time

Diffusion Models

γ	NPN–DPS	NPN–DiffPIR
0.0 (Base)	28.22	31.30
10^{-5}	28.55	31.88
10^{-4}	28.30	**31.91**
10^{-3}	28.47	30.53
10^{-2}	28.78	29.90
0.1	30.06	28.98
0.2	**30.07**	28.57
0.5	29.90	28.00

Improvements of ~1dB in different DM solvers

Deep Image Prior

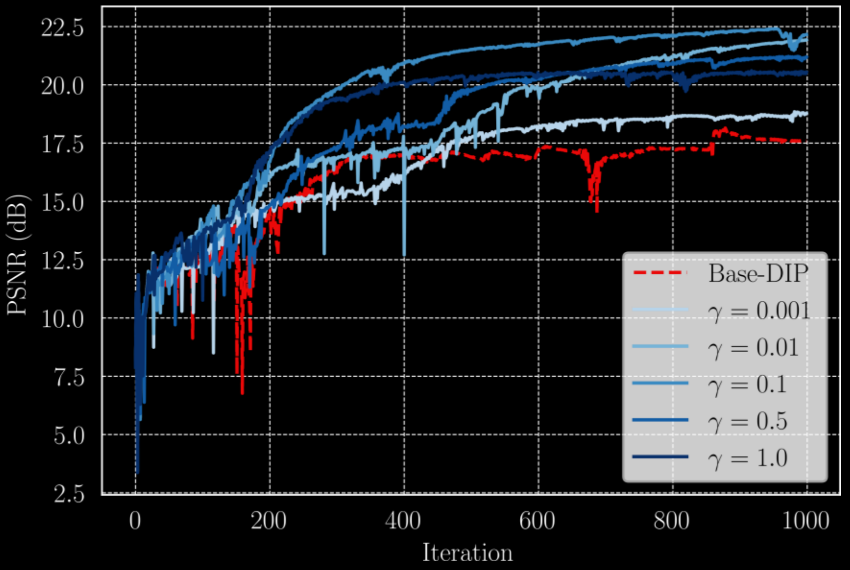

Convergence improvement in DIP and +4 PSNR gain

Compressed Sensing

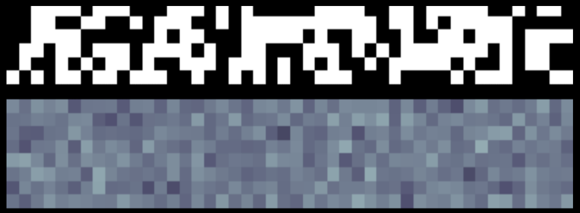

Computed Tomography

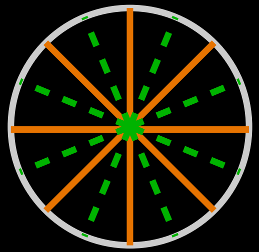

Super-Resolution

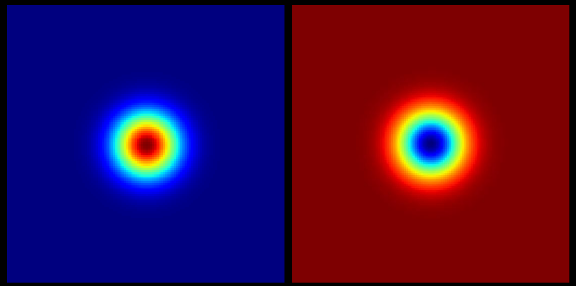

Thank You

HIGH DIMENSIONAL SIGNAL PROCESSING RESEARCH GROUP

NEURAL INFORMATION PROCESSING SYSTEMS

Universidad Industrial de Santander